Published by Institute of Physics Publishing for SISSA/ISAS

Received: *July 15, 2003*
Revised: *September 29, 2003*
Accepted: *October 10, 2003*

Single photon signals for warped quantum gravity at a linear e^+e^- collider

Santosh Kumar Rai and Sreerup Raychaudhuri

Department of Physics, Indian Institute of Technology
Kanpur 208 016, India
E-mail: skrai@iitk.ac.in, sreerup@iitk.ac.in

Abstract: We study the 'single photon' process $e^+e^- \to \gamma\nu\bar{\nu}$ with contributions due to exchange of massive gravitons in the Randall-Sundrum model of low-scale quantum gravity. It is shown that for significant regions in the parameter space, this process unambiguously highlights the resonance structure of the graviton sector. Even in the non-resonant part of the parameter space, we show that comparison with the benchmark process $e^+e^- \to \mu^+\mu^-$ can clearly distinguish signals for warped gravity from similar signals for large extra dimensions.

Keywords: Beyond Standard Model, Compactification and String Models.

JHEP10(2003)020

Contents

1. Introduction

One of the most exciting theoretical developments of recent years has been the idea that there could be one or more extra spatial dimensions and that the observable Universe could be confined to a four-dimensional hyper-surface in a higher dimensional bulk spacetime [1]. Such ideas, which fit in naturally with current ideas in superstring theory, give rise to elegant solutions to the well-known gauge hierarchy problem of high energy physics. What is even more interesting, perhaps, is the suggestion that there could be observable signals of quantum gravity at current and future accelerator experiments.

This relatively new body of ideas, commonly dubbed 'Brane World Phenomenology', bases itself on two main ideas: the concept of hidden compact dimensions [2] and the string-theoretic idea of D-branes [3]. There are two main scenarios, each having variants. One is the so-called Arkani-Hamed-Dimopoulos-Dvali (ADD) model [4], in which there are d more extra spatial dimensions, compactified on a d-torus of radius R_c each way, which, together with the four canonical Minkowski dimensions, constitutes the 'bulk' spacetime. In this scenario R_c can be [5] as large as $200\,\mu$m. However, the Standard Model (SM) fields are confined to a four-dimensional slice of spacetime, with thickness not more than $10^{-12}\,\mu$m, which is dubbed the 'brane'. If the model is embedded in a string-theoretic framework, the 'brane' is, in fact a D_3-brane, i.e. a 3+1 dimensional hyper-surface on which the ends of open strings are confined.[1] However, gravity, which is a property of spacetime itself, must be free to propagate in the bulk. As a result

[1]It is not absolutely essential to embed the model in a string theory, and the word 'brane' or 'wall' is then used simply to denote a hyper-surface or domain wall where SM fields are confined.

- Planck's constant in the bulk $\hat{M}_P$ is related to Planck's constant on the brane $M_P(\simeq\ 1.2 \times 10^{19}\,GeV)$ by $\hat{M}_P^{2+d}\ R_c^d = (4\pi)^{d/2}\ \Gamma(d/2)\ M_P^2$ which means that for $R_c \sim 200\,\mu$m, it is possible to have $\hat{M}_P$ as low as a TeV. This solves the gauge hierarchy problem simply by bringing down the scale of new physics (i.e. gravity) to about a TeV.

- There are a huge number of massive Kaluza-Klein excitations of the (bulk) graviton field, as perceived on the brane. These collectively produce effects of electroweak strength, which may be observable at current experiments and those planned in the near future [6]–[8].

A major drawback of the ADD model is that it creates a new hierarchy between the 'string scale' $\hat{M}_P \sim 1\,$TeV and the size of the extra dimensions $R_c^{-1} \sim 1\,\mu$eV. Moreover, it can be argued that the huge (compared with the Planck length) size of the extra dimensions is unstable under quantum corrections, which tend to shrink it down until $\hat{M}_P \sim R_c^{-1} \sim M_P$. This problem is brilliantly solved in the Randall-Sundrum (RS) model [9], which has grown out of the ADD model.

In the RS model, there are *two* branes — a 'visible' brane containing the SM fields and an 'invisible' brane where gravity is strong (as strong as the electroweak interaction) — embedded in a five-dimensional bulk, where the single extra dimension is a $\mathbf{S}^1/\mathbb{Z}_2$ orbifold. i.e. a circle folded about a diameter. Placing the two branes at the two orbifold fixed points $\phi = 0, \pi$, and assuming they have equal and opposite energy densities (brane tensions), which are related to a negative cosmological constant in the bulk, one obtains a 'warped' solution to the five-dimensional Einstein equations of the form

$$ds^2 = e^{-\mathcal{K}R_c\phi} g_{\mu\nu} dx^\mu dx^\nu + R_c^2 d\phi^2\,, \tag{1.1}$$

where $\mathcal{K}$ is the curvature of the fifth dimension. Gravity is strong on the invisible brane at $\phi = 0$ and weak on the visible brane $\phi = \pi$. It is now possible to choose all the fundamental energy scales in the problem in the ballpark of the Planck scale provided $\mathcal{K}R_c \simeq 12$. This moderate value reduces the 'warp factor' $e^{-\mathcal{K}R_c\pi}$ to about 10^{-16} — adequate to explain the hierarchy between electroweak and Planck scales. One thus obtains a natural solution to the hierarchy problem in this model: exponential generation of large/small numbers explains the weakness of the observed gravitational interactions. Of course, this is achieved at the cost of (a) tuning brane tensions with the bulk cosmological constant and (b) assuming negative brane-tension. It is fair to say that the RS model successfully fuses the gauge hierarchy problem with the cosmological constant problem, and presumably both have a common solution.

Phenomenologically, the RS model is rather similar to the ADD model, but there are two important differences. These are

- Each Kaluza-Klein excitation of the bulk graviton has a mass [10, 11]

$$M_n = x_n \mathcal{K} e^{-\mathcal{K}R_c\pi} \equiv x_n m_0\,, \tag{1.2}$$

where $m_0 = \mathcal{K} e^{-\mathcal{K} R_c \pi} \sim 100\,\mathrm{GeV}$ is the graviton mass scale and x_n are the zeros of the Bessel function $J_1(x)$ of order unity ($n \in \mathbb{Z}$). This means that the Kaluza-Klein gravitons have masses of a few hundred GeV, unlike the ADD case, where the masses start from $\sim 1\,\mu\mathrm{eV}$.

- Each Kaluza-Klein excitation of the bulk graviton couples to matter as [11]

$$\kappa e^{\mathcal{K} R_c \pi} = \frac{4\sqrt{\pi}}{M_P} e^{\mathcal{K} R_c \pi} \equiv \frac{4\sqrt{\pi} c_0}{m_0}\,, \tag{1.3}$$

where $\kappa = \sqrt{16\pi G_N}$ and $c_0 = \mathcal{K}/M_P \simeq 0.01 - 0.1$ is an effective coupling constant, whose magnitude is fixed by (a) naturalness and (b) requiring the curvature of the fifth dimension to be small enough to consider linearized gravity on the 'visible' brane.

RS gravitons, thus, resemble weakly-interacting massive particles (WIMPs) in most models, except for (a) the fact that there always exists a tower of graviton Kaluza-Klein modes and (b) these are spin-2 particles. In phenomenological studies of the RS model, the mass scale m_0 and the ratio c_0 may be treated as free parameters:[2] they are convenient replacements for the fundamental quantities $\mathcal{K}$ and R_c:

$$\mathcal{K} = c_0 M_P\,, \qquad R_c = \frac{1}{\pi \mathcal{K}} \log \frac{\mathcal{K}}{m_0}\,. \tag{1.4}$$

Accelerator searches for RS gravitons mainly depend on the resonant structure of graviton-mediated cross-sections. The non-observation of any such effects at LEP-2, for example, constrains $M_1 > 206\,\mathrm{GeV}$, or $m_0 > 54\,\mathrm{GeV}$. At a hadron collider, such as the Tevatron or the LHC, one looks [11] for s-channel graviton exchange contributions to simple processes like $p + p(\bar{p}) \to \ell^+\ell^-$ or $p + p(\bar{p}) \to \gamma\gamma$ or the more complicated $p + p(\bar{p}) \to$ dijets, where one should expect to see graviton resonances in the invariant mass distribution of the final state. The observation of such resonances would certainly be a signal for the RS model. However, it may not be possible to clinch the issue of whether such signals are uniquely due to RS gravitons or to some other form of new physics. The reason is simple: *any* particle exchanged in the s-channel for the above processes, such as, for example, a Z'-boson, would induce very similar signals. In order to verify that an observed resonance is indeed a graviton resonance, we need to (a) measure the position, width and height of the resonance peak, and (b) compare the angular distribution of the final states with that predicted for a spin-2 exchange in the s-channel. These may, indeed, be possible [11], despite the presence of large irreducible backgrounds at a hadron collider, which induces large errors in the width and height measurements. It is also possible that we would see signals for spin-2 exchanges without observing a clear resonance structure, in which case, one could infer either an ADD-type scenario with closely-spaced graviton states, or a RS-type scenario with smeared-out resonances. To clinch the issue, therefore, it seems natural to turn to a high-energy e^+e^- collider, where the environment is clean and to see if one can obtain an unambiguous signal for RS gravity at such a machine.

[2]The alternative choice of $\Lambda_\pi = \overline{M}_P\, e^{-\mathcal{K} R_c \pi} = m_0/\sqrt{8\pi} c_0$ instead of m_0 and of $\mathcal{K}/\overline{M}_P = \sqrt{8\pi} c_0$ instead of c_0 may also be found in the literature [11].

JHEP10(2003)020

Several studies of RS gravitons at e^+e^- colliders may already be found in the literature [12]–[14]. For example, one can have s-channel graviton exchanges in $e^+e^- \to \mu^+\mu^-, e^+e^-$ and $\gamma\gamma$. In these studies [15] it is shown that if the center-of-mass energy is run over a typical range, say 350 GeV to 1.5 TeV, one gets beautiful resonances at the masses of the RS gravitons, for a suitable choice of parameters. Conversely, if one fixes the energy and runs over the graviton mass parameter m_0, one again generates resonances whenever the condition $\sqrt{s} \simeq M_n$ is satisfied. However, one must remember that if the RS model is true, then Nature has only one value of m_0. It is also likely that the next generation e^+e^- machine will be run (like the LEP) only at certain fixed values of beam energy [16]. It is quite possible, therefore, that the actual machine energy will be an *off-resonance point* for the RS model. In such a case, the only way to excite resonances would be through 'radiative return' type reduction of the effective centre-of-mass energy as a consequence of initial-state radiation (ISR) or beamstrahlung. As this would automatically lead to a certain degree of suppression of the signal (the farther away from the resonance point, the lower the flux and hence the greater the suppression), it may not, then, be easy to distinguish graviton contributions from those due to other forms of 'new physics', such as supersymmetry or extra gauge bosons [17]. Even if such signals are observed, it would be useful to have a complementary signal from some other process, which could substantiate any claim to have seen graviton exchange.

In this article, we examine the $2 \to 3$-body process $e^+e^- \to \gamma\nu\bar{\nu}$, which is observable as a final state with a single hard transverse photon with unbalanced (missing) energy. Such states are very distinctive and are, in fact, predicted in a wide variety of models beyond the SM [18]–[20]. It is likely that some part of the experimental effort at a high-energy e^+e^- collider will be devoted to an analysis of this signal, which is simple, clean and physically interesting. The process can be thought of as a neutrino pair-production with an ISR photon, which is, however, tagged. Since this photon carries away a variable amount of energy, it is possible for the remaining system to strike a s-channel graviton resonance, just as ISR at LEP-2 has been seen to cause a 'radiative return' to the Z-boson pole. The resonant gravitons can be thought of as real particles, in which case, the basic process is the $2 \to 2$-body process $e^+e^- \to \gamma G_n$. It follows that the photon energy will be uniquely fixed by the well-known formula

$$E_\gamma = \frac{s - M_n^2}{2\sqrt{s}}\,. \tag{1.5}$$

The photon spectrum may be expected to show Breit-Wigner resonance peaks at positions given by the above equation for $n = 1, 2, \ldots$ Observation of such resonances could constitute a clear signal of RS gravity.

In practice, however, the graviton resonances need not be very narrow. As the RS graviton decay widths vary as c_0^2 (see equation 2.1), in the limit of large c_0, the decay widths are very large and the resonance peaks get smoothed out till they are no longer identifiable as resonances. One only sees a continuous photon spectrum (except for the Z-boson line, of course) with a clear excess over the SM. This is also precisely the kind of signal one would expect for the ADD model through the process $e^+e^- \to \gamma G_n$, where the ADD gravitons escape detection [6, 21]. In fact, as we shall see, the angular distribution of

JHEP10(2003)020

the photon also looks identical in both these models, and it seems difficult to disentangle the signals. We show, however, that by combining the signal for $e^+e^- \to \gamma \not{E}$ with that for the 'benchmark' process $e^+e^- \to \mu^+\mu^-$, we can still obtain a clear separation between the two models. This is an issue which has not been addressed before in the literature.

The fact that graviton widths can be large also means that we cannot, in general, evaluate the cross-section for $e^+e^- \to \gamma\nu\bar{\nu}$ using the narrow-width approximation for graviton propagators. The full machinery of a $2 \to 3$-body process must be used.

In the following section we briefly discuss the decays of RS gravitons and then go on to describe the long and cumbersome calculation of the $2 \to 3$-body process $e^+e^- \to \gamma\nu\bar{\nu}$. Our numerical results, including discovery limits in the RS model parameter space, are presented in section 3. In section 4, we discuss how to disentangle signals for the RS model in the large c_0 limit from those for the ADD scenario. We summarize our results in section 5 and relegate some important formulae to the appendix.

2. Graviton resonances and the process $e^+e^- \to \gamma\nu\bar{\nu}$

As explained above, experimental searches for RS gravitons mainly focus on the fact that they can form narrow resonances in high-energy scattering processes. A simple calculation of the graviton width yields the form

$$\Gamma_n = c_0^2 x_n^3 m_0 \sum_P \Delta_{P\bar{P}}^{(n)} , \qquad (2.1)$$

where the sum $\sum_P$ runs over all pairs of particles ($G_n \to P\bar{P}$) and the $\Delta_{P\bar{P}}^{(n)}$ are dimensionless functions of x_n and the ratios $r_P = m_P/m_0$. Their exact forms are listed in the appendix.

In figure 1, we show the region in the c_0–m_0 plane for which the graviton resonances have widths less than 10% of the mass. This is a reasonable estimate to identify a *narrow* resonance, taking likely experimental resolutions into account [16]. It is clear from the figure that, for low values of c_0, the graviton widths remain quite small, leading to identifiable resonances. This is true for $n = 1$ for a large range of the parameter space considered, unless $c_0 > 0.06$. It is likely, therefore, that the first massive graviton state will exhibit an identifiable resonance peak, a fact which forms the basis of most existing studies in the context of the LHC [22].

The situation for the next two resonances is not so simple. The figure makes it clear that we can expect fairly sharp resonance peaks for $n = 2, 3$ for values of c_0 below 0.03 and 0.02 respectively. However, as c_0 increases, these widths grow steeply and soon the resonance shape is lost. For $n > 3$ this seems to be the case, even when c_0 is small. We thus see that for suitable values of the parameters, it might be just possible to observe the first three graviton resonances in the RS model, but hardly more. In fact, most of the time, only two — or even one — resonance(s) will be identifiable. Moreover, any analysis based on identifiable resonances, such as those in ref. [22] will break down when all the resonances are wide, e.g. for $c_0 > 0.06$.

As the exact conditions for identifying a resonance at a linear collider would depend crucially on experimental resolutions, it is premature to set up a definite criterion for resonance identification. Ideally, we should use something like the Z-lineshape analysis at LEP-1, and presumably some such study will be done if and when we have data. For the present, the condition $\Gamma_n < \frac{1}{10} M_n$ was chosen purely for illustrative purposes and the following discussion is *not* predicated on any such numerical criteria.

Along with the graviton widths, in figure 1 we have also shown the results of a phenomenological analysis [15] of Tevatron dilepton data constraining the RS model parameters. The small negative-slope line inside the shaded region indicates constraints from precision data, but are not very important since they are subsumed in the region excluded by the dilepton data. We note that, for $c_0 \geq 0.01$, we already have $m_0 \geq 125\,\mathrm{GeV}$, corresponding to setting all graviton resonances heavier than about $480\,\mathrm{GeV}$. This means that RS gravitons are practically inaccessible for a $500\,\mathrm{GeV}$ linear collider and one has to consider higher energies to excite graviton resonances.

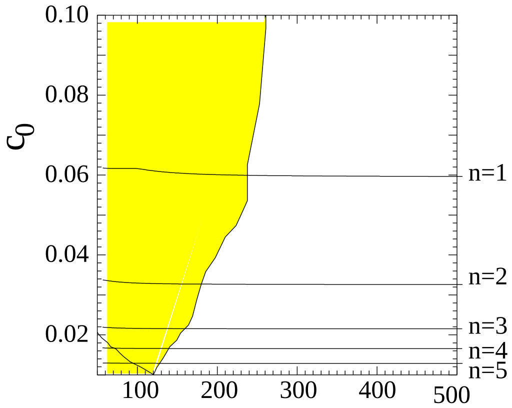

Figure 1: Illustrating the region (below the solid lines) in the parameter space of the RS model for which the graviton width remains small ($\Gamma_n < \frac{1}{10} M_n$), for the first five graviton resonances $n = 1, 2, 3, 4, 5$. The shaded region represents the constraints from dilepton production at the Tevatron Run I.

We now concentrate on the $2 \to 3$-body process

$$e^-(k_1, \lambda_1) + e^+(k_2, \lambda_2) \longrightarrow \gamma(p_1) + \bar{\nu}(p_2) + \nu(p_3)$$

which is observable as a final state with a single hard photon with unbalanced (missing) energy. Note that we display only the helicities of the initial states, as the (unobserved) helicities of the final states will be summed over.

Figure 2 shows the complete set of tree-level Feynman diagrams contributing to the process in the RS model. Diagrams 1–2, 6–9 are labeled with ν indicating a neutrino of *any* flavour, while diagrams 3–5 are specifically labeled with the electronic flavour ν_e. Feynman amplitudes corresponding to these nine diagrams are given in the appendix.

We use these amplitudes to calculate the cross-section in terms of the usual $2 \to 3$ body invariants s, s_1, s_2, t_1 and t_2. The expressions, including 36 possible interference terms, are long and messy. In the interests of brevity, we do not present them in this paper. The final cross-section was coded into a Monte Carlo event generator, which produced the numerical results. The graviton contributions require a summation over graviton Kaluza-Klein modes, parametrised by the function $\Lambda(Q^2)$, which is defined as

$$\Lambda(Q^2) = \sum_n \frac{\kappa^2 e^{2\pi \mathcal{K} R_c}}{Q^2 - M_n^2 + i M_n \Gamma_n}, \tag{2.2}$$

where n runs over all the graviton modes. We now explain briefly how the function $\Lambda(Q^2)$ is evaluated.

As mentioned above, masses of the Kaluza-Klein gravitons in the RS model vary as $M_n = x_n m_0$ where x_n are the zeroes of the Bessel function $J_1(x)$. These may be approximated by [23]

$$x_1 \simeq 1.22\pi\,, \qquad x_2 \simeq 2.23\pi\,, \qquad x_n \approx x_2 + (n-2)\pi\,. \tag{2.3}$$

However, we have seen that the width Γ_n is a complicated function of the mass M_n. If we consider Breit-Wigner resonances up to $n = N$ and simple propagator summation thereafter, we get a simplified form

$$\begin{aligned}\Lambda(Q^2) &\approx 16\pi \frac{c_0^2}{m_0^2}\left[\sum_{n=1}^{N} \frac{1}{Q^2 - M_n^2 + iM_n\Gamma_n} + \sum_{n=N+1}^{\infty} \frac{1}{Q^2 - M_n^2}\right] \\ &= 16\pi \frac{c_0^2}{m_0^4}\left[\sum_{n=1}^{N} \frac{1}{x^2 - x_n^2 + ix_n\gamma_n} + \psi\left(\frac{x_2 + x}{\pi} + N - 1\right) - \psi\left(\frac{x_2 - x}{\pi} + N - 1\right)\right],\end{aligned}$$

where $x^2 = Q^2/m_0^2$, $\gamma_n = \Gamma_n/m_0$ and ψ is the Euler digamma function, which is obtained on performing the infinite sum of the remaining terms.[3] In our numerical analysis, we determine N by the simple criterion that for $n > N$, the Breit-Wigner contribution from a single resonance should not exceed 1% of the resonance value of $\Lambda(Q^2)$. Calculated in this way, we have checked that our results closely match those of, for example, ref. [15].

3. Results and discussion

Our numerical analysis of the problem has been performed for two values of center-of-mass energy, viz., $\sqrt{s} = 1\,\mathrm{TeV}$ and $\sqrt{s} = 2\,\mathrm{TeV}$. As explained above, Tevatron data already rule out graviton resonances accessible at a 500 GeV collider, and hence we have carried out our analysis for higher energies, such as are contemplated for a variety of linear collider designs. Noting that the final state consists of a single hard isolated photon, we impose the following kinematic cuts

- The photon should have energy $E_\gamma \geq 20\,\mathrm{GeV}$.
- The photon scattering angle θ_γ should satisfy $15^0 \leq \theta_\gamma \leq 165^0$.

These ensure that the tagged photon does not arise from beamstrahlung or other similar sources [24]. Assuming 100% efficiency in photon detection (we shall see later that the actual efficiency factors cancel out), we then calculate the differential and total cross-section for both (a) unpolarised and (b) polarised beams.

Beam polarisation can be an extremely efficient tool in reduction of the SM background (diagrams 1–5 in figure 2). This is because the largest contributions to the signal arise from t-channel exchange of W-bosons in the process $e^+e^- \to \gamma\nu_e\bar{\nu}_e$ (diagrams 3–5). These diagrams are strongly suppressed if the electron (positron) beam is right (left) polarised, because of the $V - A$ nature of the W-boson coupling. This is beautifully illustrated in figure 3, where we plot the total cross-section for $e^+e^- \to \gamma\nu\bar{\nu}$ (signal-to-background

[3]Strictly speaking, the sum is not infinite, but must be cut off at the five-dimensional Planck scale. However, this is so much larger than the experimental energy that the sum is, for all practical purposes, infinite.

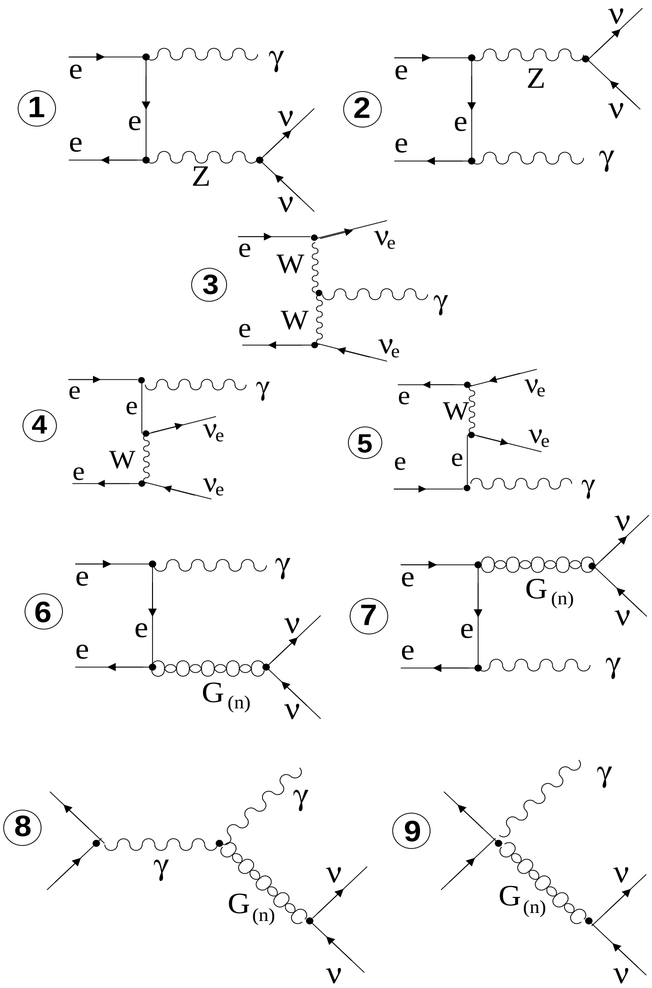

Figure 2: Feynman diagrams contributing to the process $e^+e^- \to \gamma\nu\bar{\nu}$ in the RS model. Diagrams numbered 1 to 5 are present in the SM model, while diagrams 6 to 9 involve graviton exchange. Diagrams numbered 3, 4 and 5 exist only for the electron neutrino.

ratio σ/σ^{SM}) against the center-of-mass energy $E_{cm} = \sqrt{s}$. Figure 3 actually comprises five graphs, viz., the unpolarised (0,0) case, as well as all four choices of $[sgn(P_e), sgn(P_p)]$ taking typical values [16] $|P_e| = 0.8$ and $|P_p| = 0.6$. The choice (+,-), corresponding to right (left) polarised electron (positron), produces roughly an order-of-magnitude suppression of the background and thereby throws the new physics signal into prominence in a way that cannot be achieved otherwise. For the rest of this paper, then, we concentrate on this choice. It turns out that even with the strong background suppression, the total cross-section is still in the range of a few hundred femtobarns. As we expect [16] a luminosity of at least $10\,\mathrm{fb}^{-1}$ at a linear collider, this would mean a few thousand events, and more if the high-luminosity option of $1000\,\mathrm{fb}^{-1}$ is achieved. Thus, the use of beam polarisation turns out to be an undiluted blessing.

We can study the kinematic distributions of the only two measurables: the energy E_γ and the scattering angle θ_γ of the photon. In figure 4, we display, for $\sqrt{s} = 1$ and $2\,\mathrm{TeV}$ respectively, the photon energy spectrum for both the signal and the SM background.

The dashed (black) line represents the background (note the Z-boson peak at the extreme right), while solid curves correspond to the signal for low (red) and high (blue) values of the parameter c_0. Sharp resonances are obtained with the parameter choice $c_0 = 0.01$ and $m_0 = 125\,\text{GeV}$, which is the lightest mass spectrum allowed by the Tevatron constraints. It corresponds to graviton resonances with $M_n \simeq 479, 877, 1272$ and $1665\,\text{GeV}$ for $n = 1, 2, 3$ and 4 respectively. Only the first two are kinematically accessible at a 1 TeV machine, but all four will be accessible if the centre-of-mass energy rises to 2 TeV. Observe that the resonance peaks broaden as the order $n = 1, 2, \ldots$ of the Kaluza-Klein excitation increases. For a large values of c_0, viz. $c_0 = 0.07$ (with $m_0 = 250\,\text{GeV}$, to be consistent with the Tevatron constraints — this doubles the graviton mass), the resonance line-shape merges into a continuous spectrum.

In the upper halves of the two graphs in figure 4, we display the differential cross-section for the process $e^+e^- \to \gamma + \not{E}$. The bottom halves show the same distribution, except that now we exhibit the signal-to-background (S/B) ratio. Not only does this remove the uninteresting Z-peak, but it also takes care of any radiative corrections, efficiency factors, etc, which can be written in a factorisable form.

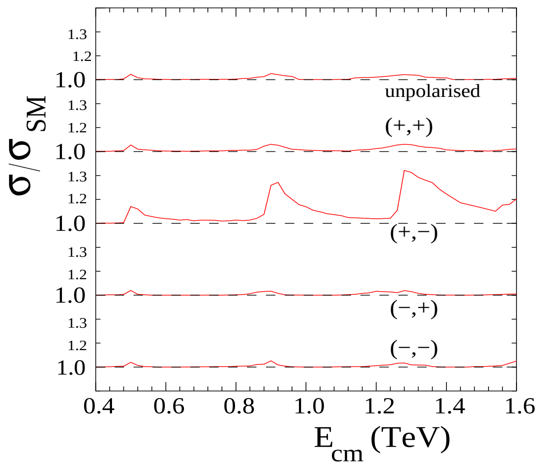

Figure 3: Illustrating the variation of the ratio between signal σ and background σ_{SM} with center-of-mass energy $\sqrt{s}$ for different choices of [sgn(P$_e$), sgn(P_p)]. Clearly the best choice is to take $\mathcal{P}_e = 0.8$ and $\mathcal{P}_p = -0.6$. The signal was calculated taking $m_0 = 125\,\text{GeV}$ and $c_0 = 0.01$, which is just allowed by the Tevatron constraints shown in figure 1.

In figure 5, we exhibit similar signal-to-background ratios for larger values of m_0, when the resonances become heavier. The first three graviton resonances lie at 766 (958), 1403 (1754), 2035 (2543) GeV respectively for $m_0 = 200$ (250) GeV. This means that only the first two resonances would be kinematically accessible, even when the centre-of-mass energy is 2 TeV. While we get sharp peaks (red curves) for lower values of c_0, when we shift c_0 close to the maximum value allowed by Tevatron data, the peaks get smeared out, except for the first one, which still retains a more-or-less recognisable shape.

Thus, we can expect one of the following possibilities.

- Case I: *Two (or more) clear resonances are seen in the photon spectrum,* or rather, in the signal-to-background ratio. This would correspond to a relatively low value of m_0 and a small value of c_0, and would constitute a strong hint of RS gravity. For confirmation, we need to check two more details. First, the peak at smaller E_γ should be lower and broader than that at larger E_γ, as illustrated in figures 4 and 5. This is because $\Gamma_n \propto x_n^3$. Secondly, the positions of the two resonances will bear a definite relation if they are due to RS gravitons. Using equation (1.5) this works out to the

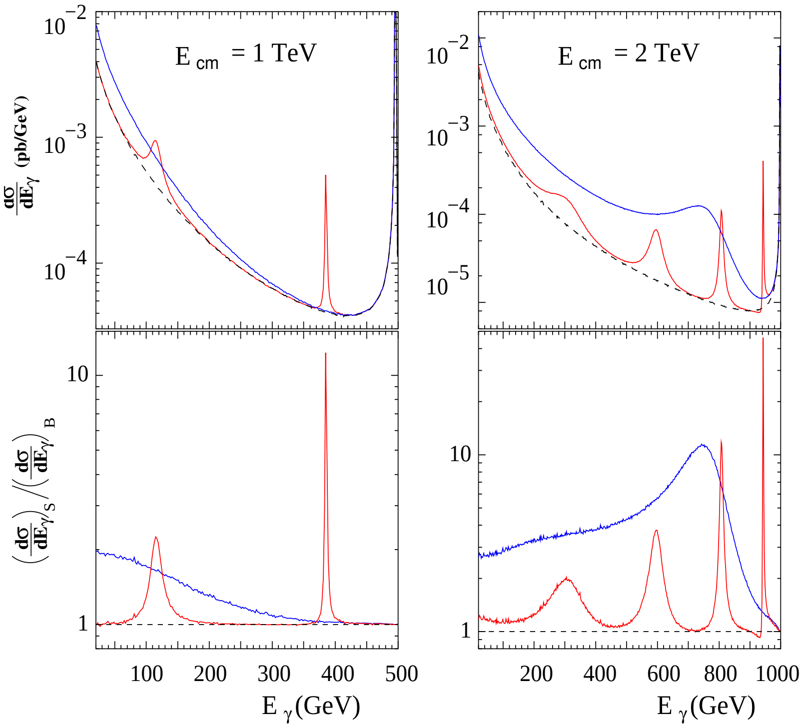

Figure 4: Energy spectrum of the tagged photon for the Tevatron-allowed parameter choices $m_0 = 125\,\mathrm{GeV}$, $c_0 = 0.01$ (red) — corresponding to narrow resonance(s) — and $m_0 = 250\,\mathrm{GeV}$, $c_0 = 0.07$(blue) — corresponding to broad, indistinct resonances. In the ordinate labels, S and B denote signal (SM plus gravitons) and background (SM only) respectively. Note that the right-most peak (almost flush with the edge of the box) in the upper graphs, which is due to the Z-boson, can be removed by taking the S/B ratio. We consider polarised beams with $\mathcal{P}_e = 0.8$ and $\mathcal{P}_p = -0.6$.

requirement that, for resonance values $E_\gamma^{(1)} > E_\gamma^{(2)}$,

$$\sqrt{\frac{\sqrt{s} - 2E_\gamma^{(1)}}{\sqrt{s} - 2E_\gamma^{(2)}}} = \frac{M_1}{M_2} = \frac{x_1}{x_2} \simeq 0.546\,. \tag{3.1}$$

It would be a very remarkable coincidence, indeed, if some other form of new physics[4] — such as, for example, two extra Z' bosons — could reproduce this ratio. Thus, if we do see two clear resonances, *satisfying the above relation*, it may be quite in order to claim this as a 'smoking gun' signal for the RS model (or a close variation).

- Case II: *One sharp resonance is seen, but no more.* If this is a graviton resonance, it will correspond to a somewhat larger value of m_0 when only the first (lightest) graviton resonance is kinematically accessible. A single resonance could also indicate the presence of some other kind of new physics, such as, for example, an extra Z' boson, or perhaps a leptophilic scalar. Of course, one can still measure the position,

[4]Barring variations of the RS model which put SM fields in the bulk [25]. The authors are grateful to K. Sridhar for pointing out this feature.

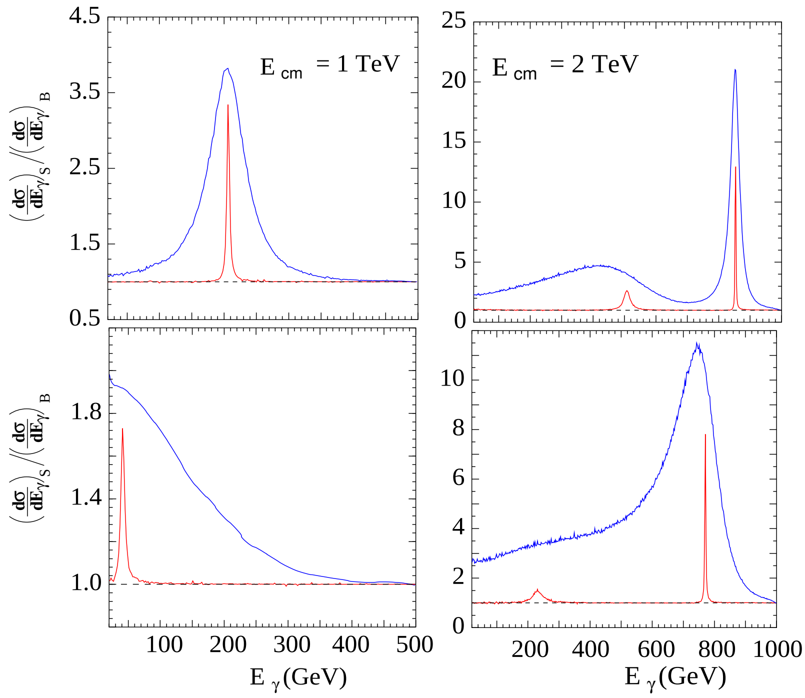

Figure 5: Illustrating the shift and disappearance of resonance peaks with increasing m_0 and c_0. The upper graphs correspond to $m_0 = 200\,\mathrm{GeV}$, $c_0 = 0.01$ (red) and $c_0 = 0.04$ (blue) while the lower ones correspond to $m_0 = 250\,\mathrm{GeV}$, $c_0 = 0.01$ (red) and $c_0 = 0.07$ (blue). Notations and conventions are similar to those used in figure 4. All parameter points are allowed by Tevatron data.

width and height of the resonance, which would be fitted with just two parameters m_0 and c_0. A consistent fit would constitute circumstantial evidence for RS gravitons, but would hardly be conclusive. However, in the case of RS gravitons, we should also expect extra contributions to 2-body final states such as $\mu^+\mu^-$, and the angular distribution of these might be useful to distinguish between different types of new physics. It is also worth mentioning that such measurements at a linear collider would be complementary to earlier measurements (including that of the spin) at the LHC and the combined evidence could be quite conclusive.

- Case III: *No resonances are seen, but large excesses in the S/B ratio are observed.* This could be due to RS gravitons with a large coupling c_0, which means smeared-out resonances, and a mass scale such that even the first resonance is inaccessible to the linear collider. However, it could also be due to various other sources, such as ADD gravitons (which form a near-continuous spectrum), or, perhaps the production of supersymmetric particles. A process like $e^+e^- \to \gamma\widetilde{\chi}^0_1\widetilde{\chi}^0_1$, where $\widetilde{\chi}^0_1$ is the (invisible) lightest neutralino, would contribute [18, 19] an excess very similar to the observed one. In this case, it may be a real challenge to determine the nature of the new physics causing this signal. In the next section we take up the issue of separating ADD versus RS graviton signals with comparable kinematic signatures. However, the comparison with supersymmetry and other types of new physics is a tricky issue, very much dependent on the choice of model parameters, and it is premature, at this point of time, to take up a detailed investigation.

- Case IV: *No excess is seen: the observed spectrum is completely consistent with the SM prediction.* This possibility would be rather disappointing, but it can hardly be ignored for that reason. In such a case, we would argue that the RS gravitons are far too heavy to be kinematically accessible to the linear collider. We would then get as bounds what we now present in figure 6 as 95% confidence level discovery limits.

In order to obtain the discovery limits shown in figure 6, we have to take into account any excess in the differential cross-section ratio shown in figures 4 and 5, *irrespective of whether a resonance is discernible or not.* To do this, we make a simple-minded χ^2 analysis of the bin-wise energy distribution of the photon, and indicate the region of the parameter space where a departure from the SM prediction would be observable at 95% confidence level. We define a χ^2 by

$$\chi^2(c_0, m_0) = \sum_i \frac{[N_i(c_0, m_0) - N_i^{SM}]^2}{N_i^{SM}} \tag{3.2}$$

assuming gaussian statistical errors[5] and defining $N_i = \mathcal{L}\sigma_i$ as the number of events expected in the ith bin. We then require χ^2 to be greater than the number expected for random gaussian fluctuations of the SM expectation. Figure 6 clearly illustrates how far a high energy linear collider can probe the RS model. Compared with the bound from Tevatron Run-I dilepton data [11, 15] we see that a linear collider can probe much larger values of m_0, i.e. graviton resonances which are many times heavier. It is worth pointing out that the mass range which can be probed at a 2 TeV machine is significantly greater than that which can be accessed at a 1 TeV machine.

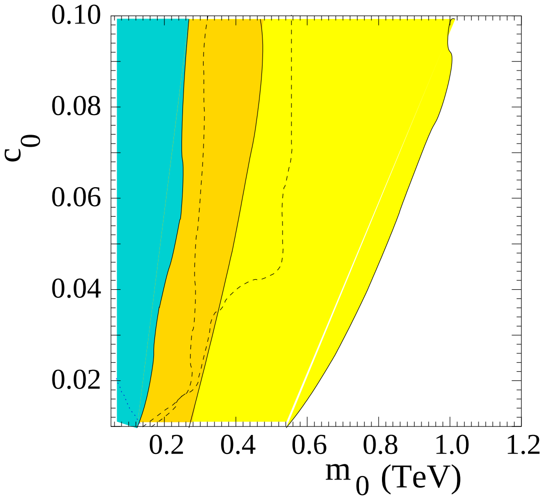

Figure 6: Discovery limits at 95% C.L. for the RS model in the c_0–m_0 plane using single-photon signals. The region shaded blue is the Tevatron bound from dileptons. The regions shaded light (dark) yellow correspond to $\sqrt{s} = (1)\ 2$ TeV and high luminosity ($\mathcal{L} = 10^3\,\mathrm{fb}^{-1}$). Broken lines on the left (right) correspond to low luminosity ($\mathcal{L} = 10\,\mathrm{fb}^{-1}$) and $\sqrt{s} = 1\ (2)$ TeV.

4. Distinguishing between RS and ADD models

We now come to the crucial issue: when the mass m_0 and/or the coupling c_0 is large, and no clear resonance structure is discernible, is it possible to distinguish between the $\gamma + \not{E}$ signal arising from RS graviton from those arising from ADD gravitons [6, 21]? We have already explained that not much can then be gained from a study of the photon energy

[5] At this stage, we consider it reasonable to ignore possible systematic errors.

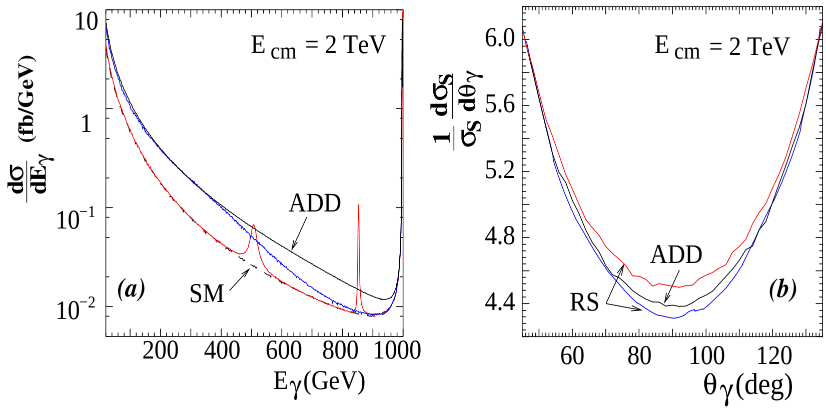

Figure 7: (a) Energy spectrum of the tagged photon showing the similarity between RS and ADD model predictions, in some regions of the parameter space. Solid red (blue) lines correspond to parameter sets $m_0 = 200\,\text{GeV}$, $c_0 = 0.01$ ($m_0 = 400\,\text{GeV}$, $c_0 = 0.09$) respectively. Solid black lines correspond to ADD model with $d = 3$ and $M_s = 5\,\text{TeV}$. The broken line shows the SM contribution. (b) Normalized angular distribution of single photons in the RS and ADD models for $\sqrt{s} = 2\,\text{TeV}$, other conventions being the same as in (a). The subscript S indicates that we consider the signal with the SM part subtracted.

spectrum. The only other observable is the photon angular distribution $d\sigma/d\theta_\gamma$. In the ADD model, the signal arises from $2 \to 2$-body processes corresponding to diagrams similar to nos. 6–9 in figure 2, but without the neutrino lines. As this involves real gravitons in the final state, there is no interference with the SM diagrams and this could be expected to lead to some difference in the angular distribution of the photon.

In figure 7, we display (a) the photon energy spectrum and (b) the (normalized) photon angular distribution at a 2 TeV collider for the following cases:

1. RS gravitons, with $m_0 = 200\,\text{GeV}$ and $c_0 = 0.01$, indicated with a solid red line;
2. RS gravitons, with $m_0 = 400\,\text{GeV}$ and $c_0 = 0.09$, indicated with a solid blue line;
3. ADD gravitons with $d = 3$ and $M_S = 5\,\text{TeV}$, indicated with a solid black line.

Considering first the energy spectrum shown in figure 7a, case 1 shows narrow resonances and may be distinguishable from the other two. However, the others differ only for $E_\gamma > 400\,\text{GeV}$, where the differential cross-section is at the level of 0.1 fb/GeV. As this is just the region where we may expect larger errorbars, it is unlikely that the energy spectrum data will provide a clear distinction between cases 2 and 3 above. Turning, therefore, to the angular distribution shown in figure 7b, we see that the same pattern repeats itself, with a clear demarcation between the resonant and non-resonant cases. In fact, unless the errorbars are very small, we may not be able to distinguish between any of these cases at all. A more detailed study, including angular resolution, is required to decide this issue, but obviously cannot be carried out at this early stage.

It appears, therefore, that a study of the process $e^+e^- \to \gamma\nu\bar{\nu}$ alone cannot clearly distinguish between the ADD and RS models, should a continuous excess in the photon spectrum be observed. However, if we consider this process *in conjunction* with a benchmark process, like $e^+e^- \to \mu^+\mu^-$, for example, we do find a marked difference. This is because the $\gamma + \not{E}$ signal arises in the ADD model from a $2 \to 2$-body process, whereas in the RS model it arises from a $2 \to 3$-body process, which is phase-space suppressed. Consequently, when the cross-sections for the two match, the ADD parameter M_S must be rather large, as is evidenced by the choice 5 TeV in figure 7. When we consider the corresponding contributions to a $2 \to 2$ body process, like $e^+e^- \to \mu^+\mu^-$, the same choice of parameters would yield a much larger cross-section for the RS model. Using this idea as a cue, in figure 8 we plot our predictions, at a 2 TeV machine, for $\sigma(e^+e^- \to \gamma \not{E})$ versus $\sigma(e^+e^- \to \mu^+\mu^-)$ for both the models in question. For the RS model, we choose two values $m_0 = 200, 400$, and vary the value of c_0 between 0.01 and 0.1, which is the expected range. For the ADD model we have varied M_S from $\sqrt{s}$ to much larger values, for $d = 3, 6$. Both sets of curves converge, in the decoupling limit, to the SM predictions (beyond the lower left corner).

A glance at figure 8 makes it obvious that a correlation plot of this nature shows a clear difference between ADD and RS models. If the actual observation point is found to lie toward the upper-left corner of the graph, one could clearly say that the signal is of RS gravity. If the observation point were to lie toward the bottom-right corner of the graph, it would be equally certain that the signal must come from ADD gravity. If, however, the point comes out close to the bottom-left corner, where the two sets of graphs merge into the SM prediction, it will be difficult to distinguish any kind of new physics effect at all. This would correspond to the Case IV in section 3.

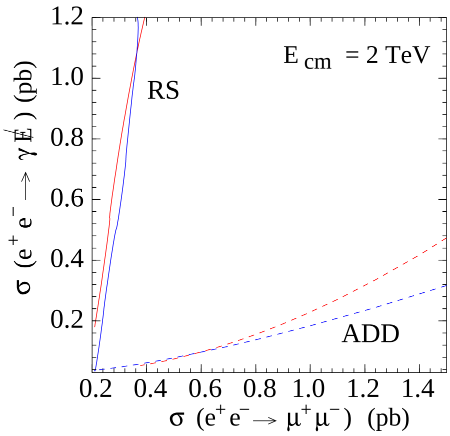

Figure 8: Correlation plot showing the cross-section for the single photon signal vis-á-vis the cross-section for muon pair-production. Broken lines correspond to the ADD model for two values of $d = 3$ (red) and 6 (blue), while solid lines correspond to the RS model for two values of $m_0 = 200$ GeV (red), 400 GeV (blue).

A correlation plot such as that shown in figure 8 could, in fact, prove more useful than merely in distinguishing between ADD and RS models. If we consider a supersymmetric model, such as the minimal supersymmetric SM, for example, we will not predict extra contributions to $e^+e^- \to \mu^+\mu^-$. In that case, the observed point will lie on the vertical axis of figure 8, and may be distinguished from the graviton contributions if the errors are small enough. Contributions from one (or more) extra Z' bosons would look similar to the RS graviton contributions, but would be distinguishable by the existence of clear resonances in the photon spectrum, since Z' widths are usually small. We have already discussed how to distinguish between graviton and Z' resonances.

Finally, it should be noted that the process considered in this article, namely $e^+e^- \to \gamma\nu\bar{\nu}$ is not the only gravitonic process at a linear collider. There could also be complementary processes [26] such as, for example, $e^+e^- \to P\bar{P}(\gamma)$ where P is any SM particle that can be tagged, which would show similar resonant behaviour due to ISR and beamstrahlung effects. A detailed investigation of these has been taken up [27].

5. Summary and conclusions

To summarize then, it is quite evident that, like supersymmetric models, solutions of the hierarchy problem which require the existence of extra hidden dimensions are here to stay. It is, therefore, of great interest to investigate their phenomenological conclusions. In this paper, we have investigated the process $e^+e^- \to \gamma\nu\bar{\nu}$ in the (minimal) Randall-Sundrum model of warped quantum gravity. This process has a clean signature, since the final observed state consists of a single hard photon with unbalanced momentum. We show that the energy spectrum of this photon could show clear resonances corresponding to massive gravitons, and discuss how these can be distinguished from other forms of new physics yielding resonances. We then consider the large-mass and large-coupling limit of the RS model, where the resonances are smeared out or inaccessible and the photon spectrum is practically indistinguishable from that predicted by the ADD model with large extra dimensions. We demonstrate that a correlation plot between the cross-sections for $e^+e^- \to \gamma \not{E}$ and a benchmark process like $e^+e^- \to \mu^+\mu^-$ can be used to make a clear demarcation, not only between signals for RS and ADD gravitons, but also between other kinds of new physics. This addresses an issue which has not been discussed in any detail before and suggests an elegant and easy-to-perform test, which uses cross-sections which are almost certain to be measured when a high-energy linear collider actually goes into operation.

Acknowledgments

This work constitutes part of the activities of the Indian Linear Collider Working Group (ILCWG) under Project No. SP/S2/K-01/2000-II, of the Department of Science & Technology, Government of India. The authors thank Sunanda Banerjee, Debajyoti Choudhury, Saurabh D. Rindani and K. Sridhar for discussions.

A. Decay width and cross-section formulae

In this appendix, we collect some useful formulae which are necessary to evaluate the graviton cross-sections discussed in the text.

Graviton decay. The dimensionless functions $\Delta^{(n)}_{P\bar{P}}$ required to calculate the graviton partial widths are listed below:

$$\begin{aligned}
\Delta^{(n)}_{\gamma\gamma} &= \frac{1}{5} \\
\Delta^{(n)}_{gg} &= \frac{8}{5} \\
\Delta^{(n)}_{WW} &= \frac{2}{5}\sqrt{1-4x_W^2}\left(\frac{13}{12}+\frac{14}{39}r_W+\frac{4}{13}r_W^2\right)\theta(x_n-2r_W) \\
\Delta^{(n)}_{ZZ} &= \frac{1}{5}\sqrt{1-4x_Z^2}\left(\frac{13}{12}+\frac{14}{39}r_Z+\frac{4}{13}r_Z^2\right)\theta(x_n-2r_Z)
\end{aligned}$$

$$\begin{aligned}
\Delta_{HH}^{(n)} &= \frac{1}{30}\left(1-4x_H^2\right)^{5/2}\theta(x_n-2r_H)\\
\Delta_{\nu\bar{\nu}}^{(n)} &= \frac{1}{10}\\
\Delta_{\ell\bar{\ell}}^{(n)} &= \frac{1}{10}\left(1-4x_\ell^2\right)^{3/2}\left(1+\frac{8}{3}r_\ell\right)\theta(x_n-2r_\ell)\\
\Delta_{q\bar{q}}^{(n)} &= \frac{3}{10}\left(1-4x_q^2\right)^{3/2}\left(1+\frac{8}{3}r_q\right)\theta(x_n-2r_q)\,,
\end{aligned}\tag{A.1}$$

where $r_P = m_P/m_0$ for every SM particle P. These formulae are consistent with those presented in ref. [7]. When using the above formulae we must remember to sum over three neutrino flavours ν, three charged leptons ℓ and six quarks q. The colour factor for quarks is already included.

Single photon production. The amplitudes corresponding to the 9 different Feynman diagrams in figure 2 are given below. Helicities of the final states are not exhibited explicitly, as these will be summed over. We have used the Feynman rules and notations given in ref. [7].

$$\begin{aligned}
M_1 &= \frac{ieg^2}{16\cos^2\theta_W}\frac{1}{(k_1-p_1)^2}\frac{1}{(p_2+p_3)^2-M_Z^2+iM_Z\Gamma_Z}\varepsilon_\mu^*(p_1)\times\\
&\quad\times\bar{v}(k_2,\lambda_2)\gamma^\alpha(c_V-\gamma_5)(\not{k}_1-\not{p}_1)\gamma^\mu u(k_1,\lambda_1)\cdot\bar{u}(p_2)\gamma_\alpha(1-\gamma_5)v(p_3)
\end{aligned}\tag{A.2}$$

$$\begin{aligned}
M_2 &= \frac{-ieg^2}{16\cos^2\theta_W}\frac{1}{(k_2-p_1)^2}\frac{1}{(p_2+p_3)^2-M_Z^2+iM_Z\Gamma_Z}\varepsilon_\mu^*(p_1)\times\\
&\quad\times\bar{v}(k_2,\lambda_2)\gamma^\mu(\not{k}_2-\not{p}_1)\gamma^\alpha(c_V-\gamma_5)u(k_1,\lambda_1)\cdot\bar{u}(p_2)\gamma_\alpha(1-\gamma_5)v(p_3)
\end{aligned}\tag{A.3}$$

$$\begin{aligned}
M_3 &= \frac{-ieg^2}{8}\frac{1}{(k_1-p_2)^2-M_W^2}\frac{1}{(k_2-p_3)^2-M_W^2}\times\\
&\quad\times\left\{(k_1-k_2-p_2+p_3)^\mu\eta^{\nu\lambda}+(k_2+p_1-p_3)^\nu\eta^{\lambda\mu}-(k_1+p_1-p_2)^\lambda\eta^{\mu\nu}\right\}\varepsilon_\mu^*(p_1)\times\\
&\quad\times\bar{v}(k_2,\lambda_2)\gamma_\lambda(1-\gamma_5)v(p_3)\cdot\bar{u}(p_2)\gamma_\nu(1-\gamma_5)u(k_1,\lambda_1)
\end{aligned}\tag{A.4}$$

$$\begin{aligned}
M_4 &= \frac{-ieg^2}{8}\frac{1}{(k_1-p_1)^2}\frac{1}{(k_2-p_3)^2-M_W^2}\varepsilon_\mu^*(p_1)\times\\
&\quad\times\bar{v}(k_2,\lambda_2)\gamma^\alpha(1-\gamma_5)v(p_3)\cdot\bar{u}(p_2)\gamma_\alpha(1-\gamma_5)(\not{k}_1-\not{p}_1)\gamma^\mu u(k_1,\lambda_1)
\end{aligned}\tag{A.5}$$

$$\begin{aligned}
M_5 &= \frac{ieg^2}{8}\frac{1}{(k_2-p_1)^2}\frac{1}{(k_1-p_2)^2-M_W^2}\varepsilon_\mu^*(p_1)\times\\
&\quad\times\bar{v}(k_2,\lambda_2)\gamma^\mu(\not{k}_2-\not{p}_1)\gamma^\alpha(1-\gamma_5)v(p_3)\cdot\bar{u}(p_2)\gamma_\alpha(1-\gamma_5)u(k_1,\lambda_1)
\end{aligned}\tag{A.6}$$

$$\begin{aligned}
M_6 &= \frac{ie}{128}\Lambda(Q^2)\frac{1}{(k_1-p_1)^2}\varepsilon_\mu^*(p_1)P_{\alpha\beta\rho\sigma}(Q)\times\\
&\quad\times\bar{v}(k_2,\lambda_2)\left\{\gamma^\alpha(k_1-k_2-p_1)^\beta+\gamma^\beta(k_1-k_2-p_1)^\alpha-2\eta^{\alpha\beta}(\not{k}_1-\not{p}_1)\right\}(\not{k}_1-\not{p}_1)\gamma^\mu u(k_1,\lambda_1)\times\\
&\quad\times\bar{u}(p_2)\left\{\gamma^\rho(p_2-p_3)^\sigma+\gamma^\sigma(p_2-p_3)^\rho\right\}v(p_3)
\end{aligned}\tag{A.7}$$

$$\begin{aligned}
M_7 &= \frac{-ie}{128}\Lambda(Q^2)\frac{1}{(k_2-p_1)^2}\varepsilon_\mu^*(p_1)P_{\alpha\beta\rho\sigma}(Q)\times\\
&\quad\times\bar{v}(k_2,\lambda_2)\gamma^\mu(\not{k}_2-\not{p}_1)\left\{\gamma^\alpha(k_1-k_2+p_1)^\beta+\gamma^\beta(k_1-k_2+p_1)^\alpha+2\eta^{\alpha\beta}(\not{k}_2-\not{p}_1)\right\}u(k_1,\lambda_1)\times\\
&\quad\times\bar{u}(p_2)\left\{\gamma^\rho(p_2-p_3)^\sigma+\gamma^\sigma(p_2-p_3)^\rho\right\}v(p_3)
\end{aligned}\tag{A.8}$$

$$\begin{aligned}
M_8 &= \frac{ie}{32}\Lambda(Q^2)\frac{1}{(k_1+k_2)^2}\varepsilon_\mu^*(p_1)P_{\alpha\beta\rho\sigma}(Q)\left\{(k_1+k_2).p_1C^{\alpha\beta\mu\nu}+D^{\alpha\beta\mu\nu}\right\}\times\\
&\quad\times\bar{v}(k_2,\lambda_2)\gamma_\nu u(k_1,\lambda_1)\cdot\bar{u}(p_2)\left\{\gamma^\rho(p_2-p_3)^\sigma+\gamma^\sigma(p_2-p_3)^\rho\right\}v(p_3)
\end{aligned}\tag{A.9}$$

$$\begin{aligned}
M_9 &= \frac{-ie}{64}\Lambda(Q^2)\varepsilon_\mu^*(p_1)P_{\alpha\beta\rho\sigma}(Q)\left\{C^{\alpha\beta\mu\lambda}-\eta^{\alpha\beta}\eta^{\mu\lambda}\right\}\times\\
&\quad\times\bar{v}(k_2,\lambda_2)\gamma_\lambda u(k_1,\lambda_1)\cdot\bar{u}(p_2)\left\{\gamma^\rho(p_2-p_3)^\sigma+\gamma^\sigma(p_2-p_3)^\rho\right\}v(p_3)\,,
\end{aligned}\tag{A.10}$$

where $c_V = 1 - 4\sin^2\theta_W \simeq 0.074$. The sum over graviton polarisations reduces, when the graviton couples to a conserved current with massless fermions, to the simple form

$$P_{\mu\nu\rho\sigma}(Q) = \eta_{\mu\rho}\eta_{\nu\sigma} + \eta_{\nu\rho}\eta_{\mu\sigma}\,, \tag{A.11}$$

where $Q = p_2 + p_3$ is the momentum carried by the graviton propagator. The tensor couplings $C^{\alpha\beta\mu\nu}$ and $D^{\alpha\beta\mu\nu}$ are given by

$$\begin{aligned} C^{\alpha\beta\mu\nu} &= \eta^{\alpha\mu}\eta^{\beta\nu} + \eta^{\alpha\nu}\eta^{\beta\mu} - \eta^{\alpha\beta}\eta^{\mu\nu} \\ D^{\alpha\beta\mu\nu} &= \eta^{\alpha\beta}p_1^\nu(k_1+k_2)^\mu - \Big\{\eta^{\alpha\nu}p_1^\beta(k_1+k_2)^\mu + \eta^{\alpha\mu}p_1^\nu(k_1+k_2)^\beta - \eta^{\mu\nu}p_1^\alpha(k_1+k_2)^\beta\Big\} - \\ &\quad - \{\alpha \leftrightarrow \beta\} \end{aligned} \tag{A.12}$$

following ref. [7]. The function $\Lambda(Q^2)$ is discussed in the text (section 2).

References

[1] K. Akama, *Pregeometry*, *Lect. Notes Phys.* **176** (1982) 267 [hep-th/0001113];
V.A. Rubakov and M.E. Shaposhnikov, *Do we live inside a domain wall?*, *Phys. Lett.* **B 125** (1983) 136;
A.T. Barnaveli and O.V. Kancheli, *The world as a membrane in a space of higher dimensionality*, *Sov. J. Nucl. Phys.* **51** (1990) 573;
I. Antoniadis, *A possible new dimension at a few TeV*, *Phys. Lett.* **B 246** (1990) 377;
I. Antoniadis, C. Muñoz and M. Quiros, *Dynamical supersymmetry breaking with a large internal dimension*, *Nucl. Phys.* **B 397** (1993) 515 [hep-ph/9211309];
I. Antoniadis, K. Benakli and M. Quiros, *Production of Kaluza-Klein states at future colliders*, *Phys. Lett.* **B 331** (1994) 313 [hep-ph/9403290].

[2] G. Nordström, *Über die Möglichkeit, das elektromagnetische Feld und das Gravitationsfeld zu vereiningen*, *Phys. Zeitschr.* **15** (1914) 504;
T. Kaluza, *On the problem of unity in physics*, *Sitz. Preuss. Akad. Wiss. Berlin* **K1** (1921) 966;
O. Klein, *Quantum theory and five-dimensional theory of relativity*, *Z. Phys.* **37** (1926) 895.

[3] See, for example, J. Polchinski, *Lectures on D-branes*, hep-th/9611050.

[4] N. Arkani-Hamed, S. Dimopoulos and G.R. Dvali, *The hierarchy problem and new dimensions at a millimeter*, *Phys. Lett.* **B 429** (1998) 263 [hep-ph/9803315];
Phenomenology, astrophysics and cosmology of theories with sub-millimeter dimensions and TeV scale quantum gravity, *Phys. Rev.* **D 59** (1999) 086004 [hep-ph/9807344];
I. Antoniadis, N. Arkani-Hamed, S. Dimopoulos and G. Dvali, *New dimensions at a millimeter to a Fermi and superstrings at a TeV*, *Phys. Lett.* **B 436** (1998) 257 [hep-ph/9804398].

[5] J.C. Long *et al*, *Upper limits to submillimeter-range forces from extra space-time dimensions*, *Nature*, **421** (2003) 922.

[6] G.F. Giudice, R. Rattazzi and J.D. Wells, *Quantum gravity and extra dimensions at high-energy colliders*, *Nucl. Phys.* **B 544** (1999) 3 [hep-ph/9811291].

[7] T. Han, J.D. Lykken and R.-J. Zhang, *On Kaluza-Klein states from large extra dimensions*, *Phys. Rev.* **D 59** (1999) 105006 [hep-ph/9811350].

JHEP10(2003)020

[8] For a very readable review, see, for example, Y.A. Kubyshin, *Models with extra dimensions and their phenomenology*, hep-ph/0111027.

[9] L. Randall and R. Sundrum, *A large mass hierarchy from a small extra dimension*, *Phys. Rev. Lett.* **83** (1999) 3370 [hep-ph/9905221].

[10] W.D. Goldberger and M.B. Wise, *Bulk fields in the Randall-Sundrum compactification scenario*, *Phys. Rev.* **D 60** (1999) 107505 [hep-ph/9907218].

[11] H. Davoudiasl, J.L. Hewett and T.G. Rizzo, *Phenomenology of the Randall-Sundrum gauge hierarchy model*, *Phys. Rev. Lett.* **84** (2000) 2080 [hep-ph/9909255].

[12] T.G. Rizzo, *Unique graviton exchange signatures at linear colliders*, hep-ph/0209065; *Extra dimensional signatures at clic*, *eConf* **C010630** (2001) P301 [hep-ph/0108235].

[13] P. Das, S. Raychaudhuri, S. Sarkar, *HERA constraint on warped quantum gravity*, *J. High Energy Phys.* **07** (2000) 050 [hep-ph/0002079].

[14] D.K. Ghosh and S. Raychaudhuri, *Testing the Randall-Sundrum model at a high-energy e^- e^- collider*, *Phys. Lett.* **B 495** (2000) 114 [hep-ph/0007354].

[15] H. Davoudiasl, J.L. Hewett and T.G. Rizzo, *Experimental probes of localized gravity: on and off the wall*, *Phys. Rev.* **D 63** (2001) 075004 [hep-ph/0006041].

[16] ECFA/DESY LC Physics Working Group collaboration, J.A. Aguilar-Saavedra et al., *Tesla technical design report part III: physics at an e^+e^- linear collider*, hep-ph/0106315; NLC ZDR Design Group and NLC Physics Working Group collaboration, S. Kuhlman et al., *Physics and technology of the next linear collider: a report submitted to snowmass '96*, hep-ex/9605011.

[17] T.G. Rizzo, *More transverse polarization signatures of extra dimensions at linear colliders*, *J. High Energy Phys.* **06** (2003) 021 [hep-ph/0306283].

[18] K. Grassie and P.N. Pandita, *Production of photinos in $e^+e^- \to \gamma$ photino photino*, *Phys. Rev.* **D 30** (1984) 22.

[19] A. Datta, A. Datta and S. Raychaudhuri, *Observing virtual LSPS at lep-2*, *Phys. Lett.* **B 349** (1995) 113 [hep-ph/9411435]; *Virtual lsps at e^+e^- colliders*, *Eur. Phys. J.* **C 1** (1998) 375 [hep-ph/9605432].

[20] A. Ghosal, A. Kundu and B. Mukhopadhyaya, *Probing gauge-mediated supersymmetry breaking through polarized electron beams in an e^+e^- collider*, *Phys. Rev.* **D 56** (1997) 504 [hep-ph/9612321]; *Gauge-mediated supersymmetry breaking signals in an electron photon collider*, *Phys. Rev.* **D 57** (1998) 1972 [hep-ph/9709431].

[21] E.A. Mirabelli, M. Perelstein and M.E. Peskin, *Collider signatures of new large space dimensions*, *Phys. Rev. Lett.* **82** (1999) 2236 [hep-ph/9811337].

[22] B.C. Allanach *et al*, *Exploring small extra dimensions at the large hadron collider*, *J. High Energy Phys.* **12** (2002) 039 [hep-ph/0211205];
P. Traczyk and G. Wrochna, *Search for Randall-Sundrum graviton excitations in the cms experiment*, hep-ex/0207061.

[23] See, for example, M. Abramowitz and I.E. Stegun, *Handbook of mathematical functions*, US National Bureau of Standards, Washington 1972.

[24] C.H. Chen, M. Drees and J.F. Gunion, *Searching for invisible and almost invisible particles at $e\ +e\ -$ colliders*, *Phys. Rev. Lett.* **76** (1996) 2002 [hep-ph/9512230].

JHEP10(2003)020

[25] T.G. Rizzo, *Probing universal extra dimensions at present and future colliders*, in *Les Houches 2001, Physics at TeV colliders*, 2001, p.245.

[26] See, for example, T.G. Rizzo, *Unique identification of graviton exchange effects in e^+ e^- collisions*, *J. High Energy Phys.* **10** (2002) 013 and references therein

[27] R.M. Godbole, S.K. Rai and S. Raychaudhuri, work in progress.